

Numerical method of active thermography for the reconstruction of back wall geometry

Regina RICHTER¹, Christiane MAIERHOFER¹, Marc KREUTZBRUCK¹, Meinhard SCHILLING²

¹ Federal Institute for Materials Research and Testing; Berlin, Germany

Phone: +49 30 81044184, Fax: +49 30 81041847; e-mail: regina.richter@bam.de,
christiane.maierhofer@bam.de, marc.kreutzbruck@bam.de

² Technische Universität Braunschweig; Braunschweig, Germany; e-mail: m.schilling@tu-braunschweig.de

Abstract

The paper presents numerical methods to detect and classify defects and inhomogeneities by means of active thermography. The objective is to determine the wall thickness of structure elements with an inaccessible back wall, for example, of pipes or containers. As test specimens we used approximately 2 cm thick PVC samples with spatial variations in the back wall geometry. Flash lamps provided the heating. To know the thickness of the wall, we used two inversion methods and compared the results achieved. One is an iterative echo defect shape method and already tested on steel test specimens with good reconstruction results. The second one is the Levenberg-Marquardt method, applied here to thermographic data for non-destructive testing. Since data capturing using active thermography and the presented numerical methods can easily be automated, the combination of these two procedures is a promising approach providing a broad area of application.

Keywords: Impulse-thermography, inversion, Levenberg-Marquardt method, echo defect shape, defect shape reconstruction.

1. Introduction

Thermography has recently been established along with other non-destructive methods for structure element characterisation like ultrasonic, magnetic field and eddy current methods. The advantage of thermography is that contrary to the other methods it is contact-free and directly image-guided and therefore attains higher measurement velocities and higher resolutions and can be automated easier. There exist several thermographic methods enabling to detect quantitative parameters such as the geometry of a structure element or its thermal characteristics. The impulse-thermography (PT) is popular because it allows inspecting the structure very quickly: the duration of a short thermal stimulation pulse ranges from a few milliseconds for high-conductivity material (such as metal) to a few seconds for low-conductivity specimens (such as GFRP, concrete). In order to heat a structure element, we can apply visible and infrared radiation (laser, halogen lamps, flash lamps), but depending on the material also microwaves, chemical processes, or electromagnetic induction might be suitable. The application of flash lamps is common: This technique consists of a short light impulse radiating from the flash lamp and heating up the structure element. By analysing the surface temperature we can detect inhomogeneities: the surface temperature decays as long as the heat can flow off into the interior. The time needed for the heat diffusion is a hint for the wall thickness. Concrete structures were assessed using pulse-phase-methods [1], where the temperature is analysed in the frequency domain. To enhance the resolution for a given depth, lock-in thermography was considered and compared with impulse-thermography, see [2] for delaminations of Cu solder connections.

The aim of reconstructions is to enhance detection and classification of defects and inhomogeneities and to get quantitative information, e.g. of the wall thickness, of voids or of material properties like thermal diffusivity. Complex physical laws, like the heat equation, are here involved, and more informations of the data are evaluated: not only the temperature for a specific time, but for a whole time interval. Starting from the 1D thermal wave model, reconstructions of back walls of metal test specimens are shown by Lugin/Netzelmann [3],

Vavilov/Grinzato/Marinetti [4],[5],[6], and Götschel et al. [7] to detect corrosion. Even if these methods partly incorporate 2D/3D effects, the heat equation itself is always solved in 1D. For more accuracy regarding the lateral effects in 2D/3D, optimisation methods (e.g. least squares methods) are applied, considering the 2D/3D heat equation as a nonlinear ill-posed problem [8]. Reconstructions using least squares methods are shown in Banks et al. [9], Marcuzzi [10], and Bison [11]. Besides optimisation methods, inversion methods are an alternative approach to nonlinear ill-posed problems; but systematic studies of inversion methods applied for thermographic non-destructive testing are still lacking. We reconstructed back wall geometries using the iterative echo defect shape method - a fixed point iteration based on the 1D thermal wave model and successfully tested by Lugin for a steel test specimen [3]. The results for our PVC test specimen were enhanced by applying an inversion method, the Levenberg-Marquardt method (LM), which is one of the classical regularisation methods for nonlinear ill-posed problems and is broadly applied in geophysics and in many other fields. The well reconstruction of the back wall broadened the theoretical scope of impulse-thermography.

2. Numerical methods for reconstructing the wall thickness

For yielding the quantitative information of the wall thickness, we tested two inversion methods: the iterative echo defect shape method and the Levenberg-Marquardt method. Figure 1 presents the general principle of the complete inversion procedure.

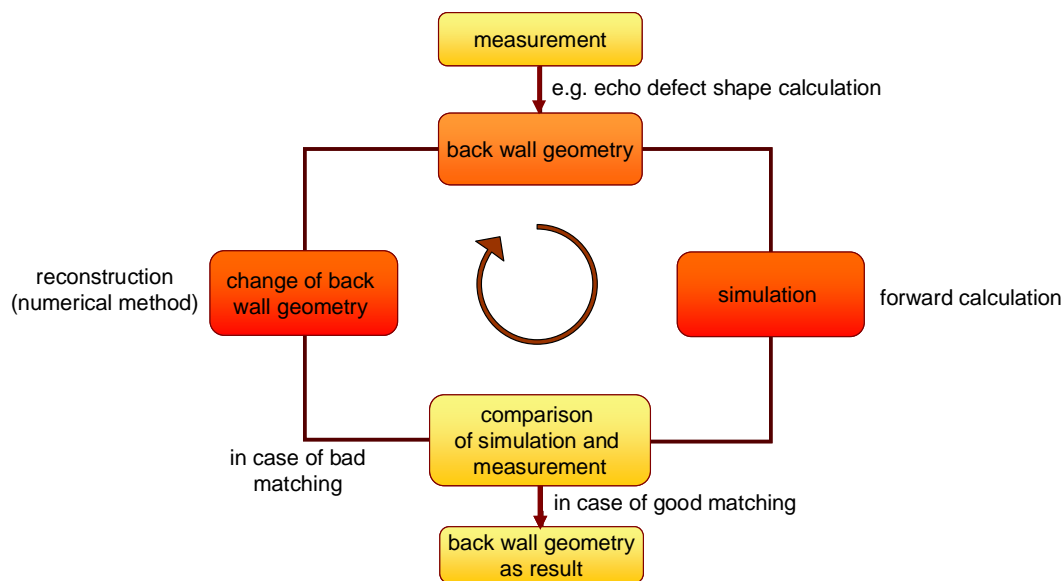


Figure 1. Complete inversion procedure

First, we are performing measurements yielding experimental data, from which we are calculating an initial back wall geometry. Second, we simulate the temperature devolution (forward calculation) for the assumed structure, details s. section 3.2 Simulation. Third, by comparing the results of simulation with the experimental data, we change the back wall geometry by an inversion method (reconstruction). The forward calculation and the reconstruction are done iteratively. Finally, the circle is stopped as soon as the simulation and the experimental data are matching well, i.e. when the sum of the quadratic fault (pointwise in time and space) is below a defined value. Thus, we successfully reconstructed the back wall

from thermographic data. Within the algorithms, the maximum possible sample thickness was fixed to 2 cm.

2.1 Iterative echo defect shape method

The first inversion method applied here is the iterative echo defect shape method (iterative EDS). As described above, this procedure was successfully applied to steel test specimens with good reconstruction results, see Lugin et al. [3]. Here, the analytical 1D solution for the heat equation for a specimen with semi-infinite thickness which is exposed to a Dirac delta pulse heating on the front is calculated. The 1D thermal wave model declares, that for a specimen with given finite thickness y , reflection of the thermal wave on the back occurs and leads to a temperature increase at the front which is equal to the temperature of the semi-infinite specimen at the depth $2y$. By considering the relative temperature increase $T_{rel}(t) = (T(t) - T_{defect-free}(t)) / T_{defect-free}(t)$ with respect to a defect free area, the specimen depth can be evaluated by

$$y = \left(-\frac{kt}{\rho c} \ln(T_{rel}(t)) \right)^{\frac{1}{2}}, \quad (1)$$

which is known as the echo defect shape (EDS), with t being the time elapsed after the delta pulse heating, and given material parameters thermal conductivity k , density ρ , and specific heat capacity c . To apply EDS (1), we predisposed a benchmark for T_{rel} , which on the one hand was big enough to cover the signal-to-noise-ratio and which was small enough, such that T_{rel} of defects hit the bench. Apparently, we oversaw small defects, as its relative temperature increase T_{rel} slipped under the benchmark. Here we set the thickness at 2 cm (*a priori* knowledge). The accuracy of EDS was best for the benchmark $B = 0.24$, evaluating data of 20 experiments. For quantifying the accuracy, we expressed the error on average by the arithmetic mean:

$$error = \frac{\sum_{i=1}^n |r^i - y^i|}{n}, \quad (2)$$

where r^i was the thickness of the real geometry (at the i -th front point), y^i the calculated EDS and n the number of front points.

The iterative EDS, which aims to enhance the EDS, consists of the fix point equation

$$y_{k+1} = y_k + (y_1 - \tilde{y}_k), \quad (3)$$

where y_1 is the EDS calculated directly from the experimental data and \tilde{y}_k is the EDS of the simulated temperature devolution for the assumed wall y_k (details s. section 3.2 Simulation). This algorithm is yielded from the observation, that the EDS is too thin for 2D reconstructions due to the lateral flow. This algorithm is fast, but the experimental data influences directly only y_1 (not y_k for $k \geq 2$).

2.2 Levenberg-Marquardt method

The second numerical method of inversion, the Levenberg-Marquardt method (LM) is one of the classical regularisation methods for nonlinear ill-posed problems and is broadly applied e.g. in geophysics [12]. LM is based on an iterative Newton type method:

$$\begin{array}{c}
 \begin{array}{cccc}
 \text{back wall} & & \text{experimental} & \\
 \text{geometry} & \text{sensitivity} & \text{data} & \text{simulation} \\
 \downarrow & \downarrow & \downarrow & \downarrow \\
 \end{array} \\
 y_{k+1} = y_k + F'(y_k)^+ \cdot (T - F(y_k)) \\
 \downarrow \\
 \text{new back wall} \\
 \text{geometry}
 \end{array} \tag{4}$$

The special case for a real function is known as Newton iteration and converges quadratically, if the initial value is “close enough” to zero. The vector function F labelled the relation of a given specimen geometry y (i.e. the wall thickness) to the temperature devolution T (in space and time on the front wall), according to laws like heat equation and convection. The derivative of F was a non-quadratic matrix, which was pseudo-inverted and was then marked by a high +. As an initial geometry for the iteration, we applied EDS (1) on the experimental data. In each iteration step, the comparison of simulated and measured temperature data ($T - F(y_k)$) yielded a correction of the back wall. Especially the sensitivity of the simulation concerning tiny changes in the back wall geometry, i.e. the derivative $F'(y_k)$, defines the correction.

For determining the sensitivity, there are various possibilities. For the first iteration, we chose the difference method, as it is an accurate method. Crucial for the good performance of the algorithm was, that we defined the infinitesimal variation of the geometry, which is needed for the difference method, as a triangle of -1/10 mm depth and 20 mm width. For the latter iterations, we chose Broyden’s method [13], as it provided time efficiency. Resulting from the secant equation, a known sensitivity defines the sensitivity in the following iteration step. As it requires no further simulation, Broyden’s method delivered results after a few seconds instead of several hours. Tests with synthetic data (i.e. simulated, noise-free data) backed our choice of Broyden’s method, as the performance was similar. For mitigating the disturbing impact of noise after our adjustment to this application, the iterative Newton type method has to be regularised.

The Tikhonov regularisation [14],[8] is well-known as a classical regularisation for its so-called mathematical optimality. The iterative Newton type method combined with Tikhonov regularisation is known as Levenberg-Marquardt method:

$$y_{k+1} = y_k + [F'(y_k)^T \cdot F'(y_k) + \alpha \cdot I]^{-1} \cdot F'(y_k)^T \cdot (T - F(y_k)), \tag{5}$$

where I is the identity matrix, α a regularisation parameter adjusted to the signal-to-noise-ratio, and T labels the transposed matrix. We optimised the regularisation to our application by choosing $\alpha = 150$ after comparing their performances. On the one hand, LM is generally much slower than iterative EDS, on the other hand, LM is less dependent on the thermal wave model, i.e. LM is directly based on the law of heat equation, and the experimental data influences directly the reconstruction in each iteration step.

3. Evaluation

3.1 Test specimen and experimental setup

The material of our test specimens was black hard-PVC, due to its excellent emissivity and absorption coefficient of 0.96 without any surface treatment. The inaccessible defect was represented by different notch shapes at the back of PVC specimens. Figure 2 and 3 show the first PVC specimen with the angle 120° ; the second specimen has an angle of 90° .

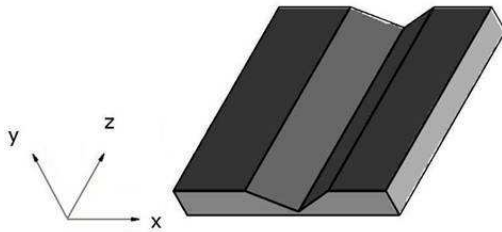


Figure 2. PVC specimen in 3D. The defect was imitated by a triangular notch shape.

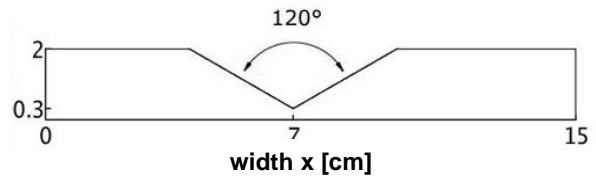


Figure 3. Profile of the PVC specimen. The wall thickness varied from 2 cm to 0.3 m.

We measure in reflection: On the defect free front of the test specimen, we temporarily heated up with two flash lamps (about 2.5 ms) and measured the temperature distribution during and after heating as a function of time using an infrared camera, Figure 4 shows the experimental set-up, and figure 5 shows an example of the recorded temperature on the test specimen 60 s after the flash; we subtracted a thermogram recorded before heating for minimising temperature errors due to reflection on the test specimen. We see a contrast of 0.7 K between non-defect areas (green) and warmer defect areas (red). By evaluating this spatial and temporal temperature distribution, we reconstructed quantitative information of the back wall geometry.

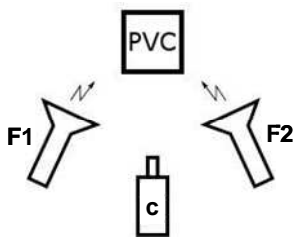


Figure 4. Sketch of the experimental set-up in reflection configuration. F1 and F2 are the flash lamps and c the infrared camera.

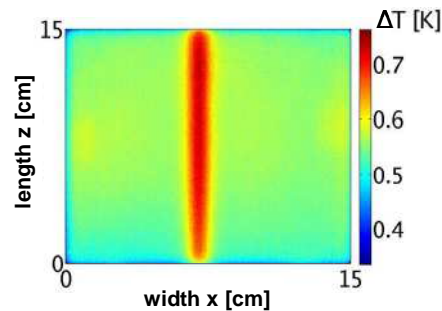


Figure 5. Thermogram of the heated PVC specimen 60 s after the flash. The infrared photography shows the temperature difference of the PVC specimen to the ambient temperature.

Here, an InSb camera was combined with a lens with a focal length of 100 mm. By using a band pass filter, the system was sensitive between 3.8 and 7.0 μm . The array size of the camera was 640 x 512, but only a frame size of about 475 x 475 pixels was analysed here. The frame rate was 93 Hz, after averaging 93 frames, the frame rate resulted to 1 Hz. For reducing the signal-to-noise ratio, we averaged 10 measurements for each specimen and averaged along the notch direction (along z). For guaranteeing a more homogenous heating, we switched the position of flash F1 and F2 after 5 measurements.

3.2 Simulation

The simulation of the experiment played a crucial role in both inversion methods (forward calculation). We solved the heat equation applying the Finite-Element-Method (FEM) in 2D. As a result, we obtained the temperature distribution on the surface and inside the test specimen. The simulation software COMSOL Multiphysics needed 3.5 min for the 2D forward calculation (PC with 16 cores). In Figure 6, we see the calculated temperature in the interior of the 2D test specimen 60 s after the flash, modelled by a pulse heating with time duration $\Delta t = 170$ ms on the front $y = 0$ cm. For enhancing the reconstruction of the back wall geometry, the spatial distribution of the flash in the experiment, which was defined by the first frame showing a heated specimen, determined the flash in the simulation; same holds for the ambient temperature, which was defined by the mean temperature of the specimen at a thermogram recorded before heating. The mesh counts about 30,000 knots, which results in a much thinner net on the front as the net of 475 pixels of the experimental data.

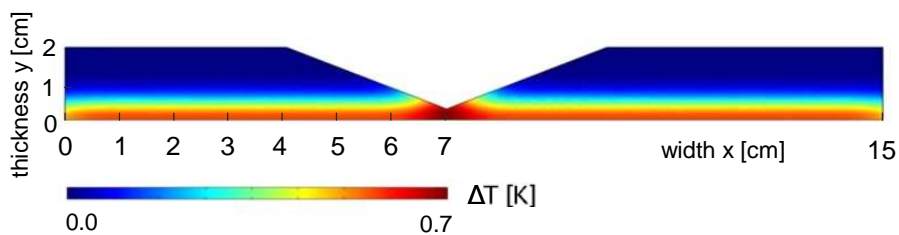


Figure 6. Simulation of the temperature with COMSOL for $t = 60$ s. The energy, which had been applied on the front $y = 0$, has heated up the interior. The warmest point of the test specimen was at the front at $x = 7$ cm, where the test specimen is thinnest (0.3 cm thickness).

3.3 Evaluation of the iterative echo defect shape and the Levenberg-Marquardt method

We evaluated both methods for its reconstruction performances for supporting points with 1 mm distances, a requirement for a fine resolution. For both methods, we used the a priori knowledge, that the wall thickness is 2 cm or less.

As the iterative EDS is already tested for thermographic NDT, we expected successful reconstructions. But in this case, iterative EDS diverged, i.e. the reconstruction was worse than the initial geometry, s. figure 7. Contemplating on the initial geometries, the sudden step from defect free, i.e. $y = 2$ cm, to $y = 0.8$ cm was due to the benchmark method of EDS (1). With LM, we found an alternative method, which converged: The method enhanced the initial geometry, s. figure 8. At the LM reconstructions, the similar sudden step was due to the insensitivity for thick initial geometry areas (stemming from the finite difference method for diffusion processes). For quantifying the accuracy of the reconstruction, we expressed the *error* on average (2) by the arithmetic mean. For the first specimen PVC 120°, the reconstructions and its *error* hinted at the general LM potential for the thermographic NDT application in opposition to the iterative EDS.

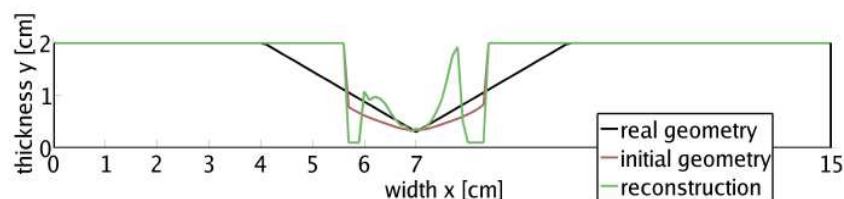


Figure 7. Divergence using iterative EDS for PVC 120° with resulting error = 1.70 mm.

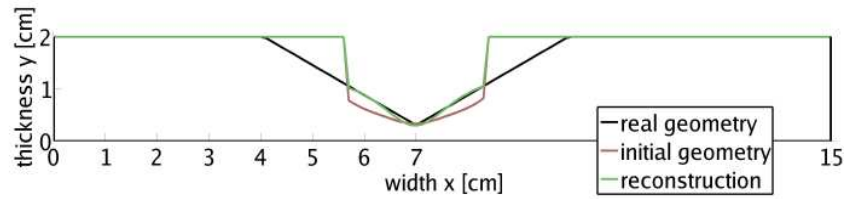


Figure 8. Convergence using LM for PVC 120° with resulting error = 1.02 mm. The thickness of the test specimen was well reconstructed for defect depth smaller than 1 cm and defect free area.

For the second specimen PVC 90°, even if there were no obvious changes in the geometry, the *error* yet hinted at the preference of LM. The iterative EDS failed, as the *error* grew, figure 9, but LM enhanced continuously – although slightly – the back wall geometry, figure 10.

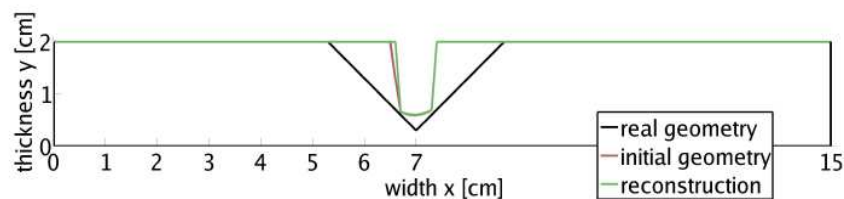


Figure 9. Divergence using iterative EDS for PVC 90° with resulting error = 1.28 mm.

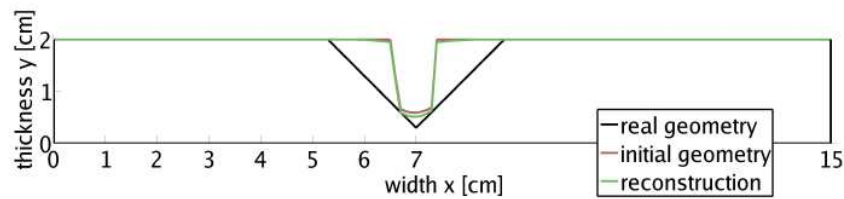


Figure 10. Convergence using LM for PVC 90° with resulting error = 1.17 mm.

Divergence occurs when the initial geometry is “too far” from the real geometry. The EDS with benchmark $B = 0.24$ was “good enough” as initial geometry for LM, but not for iterative EDS. This was visible mostly for PVC 120°, as the defect is bigger, concerning its volume or its diameter per depth. PVC 90° showed a limit of LM with presented parameters. The costs for LM were about 11 h, as several simulations of temperature devolution had to be calculated for the sensitivity.

4. Conclusion and further work

We successfully reconstructed the back wall geometry of a PVC test specimen in 2D from experimental thermographic data. The quantitative information about the slab thickness - especially fine resolution per mm - is important for non-destructive testing methods. We evaluated the reconstruction performance of the two methods. Contrary to our expectations, the iterative echo defect shape method (iterative EDS), which performs well for steel samples [1], performed poorly for the tested PVC samples. With Levenberg-Marquardt method (LM), we fortunately found an alternative method, which enhanced the initial geometry EDS. Especially the defects up to 10 mm deep could be reconstructed well. The wall thickness of the first PVC specimen was found ± 1.0 mm on average. The second specimen with a smaller defect was a challenge for LM. Considering the benchmark effect of EDS for LM, we are going to aim reconstructions using smaller benchmarks even if this yields a worse initial geometry. We assume that the LM will nonetheless profit: we might outsmart the challenging effect of diffusion by a partly too thin initial geometry instead of a too thick initial geometry. In further work, to assure the performance for various applications, we are going to test the

algorithms for more back wall geometries. We are going to apply alternative algorithms like the conjugate gradient method as we aim to reduce the calculation time.

Acknowledgements

We thank Dr. M. Ziegler, Dipl.-Ing. M. Röllig, Dipl.-Ing. H. Steinfurth, and Dr. R. Krankenhagen from BAM 8.46, Germany, for their assistance in the experimental work and we thank Dr. G. Kervalishvili, Dr. M. Blome, Dipl.-Math. S. Götschel from ZIB, Germany, Dipl.-Math. J. Offtermatt and Prof. B. Kaltenbacher from University Graz, Austria, for their helpful suggestions for the numerical implementation.

References

1. C. Maierhofer, R. Arndt, M. Röllig, C. Rieck, A. Walther, H. Scheel, B. Hillemeier, 'Application of impulse-thermography for non-destructive assessment of concrete structures', *Cement and Concrete Composites* Vol 28, pp 393-401, 2006
2. C. Maierhofer, M. Röllig, H. Steinfurth, M. Ziegler, M. Kreuzbruck, C. Scheuerlein, S. Heck, 'Non-destructive testing of Cu solder connections using active thermography', submitted to *NDT&E*, 2011
3. S. Lugin, U. Netzelmann, 'A defect shape reconstruction algorithm for pulsed thermography', *NDT&E International* Vol 40, pp 220-228, 2007
4. V. Vavilov, E. Grinzato, P.G. Bison, S. Marinetti, M.J. Bales, 'Surface transient temperature inversion for hidden corrosion characterisation: theory and applications', *Int. Journal Heat & Mass Transfer* Vol 39, pp 355-371-255, 1996
5. E. Grinzato, V. Vavilov, P.G. Bison, S. Marinetti, 'Hidden corrosion detection in thick metallic components by transient IR thermography', *Infrared Physics Technology* Vol 49, pp 234-238, 2007
6. S. Marinetti, V. Vavilov, 'IR thermographic detection and characterization of hidden corrosion in metals: General analysis', *Corrosion Science* Vol 52, pp 865-872, 2010
7. S. Götschel, M. Weiser, C. Maierhofer, R. Richter, M. Röllig, 'Fast defect shape reconstruction in travel time pulsed thermography', to be printed in *NDTMS*, 2011
8. H. W. Engl, M. Hanke, A. Neubauer, 'Regularization of Inverse Problems', Kluver, 1996
9. H. T. Banks, F. Kojima, W.P. Winfree, 'Boundary estimation problems arising in thermal tomography', *Inverse Problem* Vol 6, pp 879-921, 1990
10. F. Marcuzzi, S. Marinetti, 'Efficient reconstruction of corrosion profiles by infrared thermography', *Journal of Physics: Conference Series* Vol 124, 012033, 2008
11. P. Bison, M. Ceseri, G. Inglese, 'Detecting hidden defect on thin metallic plate', *Proceedings of the 10th International Conference on Quantitative Infrared Thermography QIRT 10*, 2010
12. M. Blome, 'Efficient measurement and data inversion strategies for large scale geoelectric surveys', Dissertation ETH 2009
13. B. Kaltenbacher, A. Neubauer, O. Scherzer, 'Iterative Regularization Methods for Nonlinear Ill-Posed Problems', de Gruyter, 2008
14. A. Rieder, 'Keine Probleme mit Inversen Problemen', Vieweg, 2003